

Two-Step Hybrid Multiuser Equalizer for Sub-Connected mmWave Massive MIMO SC-FDMA Systems

R. Magueta¹, D. Castanheira¹, A. Silva¹, R. Dinis², and A. Gameiro¹.

¹ Instituto de Telecomunicações (IT) and DETI, University of Aveiro, Portugal

² Instituto de Telecomunicações (IT) and Faculdade de Ciências e Tecnologia, Univ. Nova de Lisboa, Portugal

Abstract – Most of the works consider hybrid fully connected architectures to overcome the constraints of millimeter wave massive MIMO systems. However, these schemes require a one-to-one connection between the RF chains and antennas. In this paper we propose a two-step broadband multiuser equalizer for hybrid sub-connected architectures, which is a more realistic approach for practical systems. The low-complexity user-terminals employ only analog precoders computed from the knowledge of the average angle of departure of each cluster, which is constant over the bandwidth. At the receiver side, we design a hybrid multi-user equalizer by minimizing the average bit-error-rate. A two-step approach is considered, where the analog part is constant over the iterations due to hardware constraints and the digital part is iterative. The analog part is also constant over all subcarriers while the digital part is computed on a per subcarrier basis. The proposed sub-connected based equalizer is compared with the fully connected counterpart. The results show that the performance of the proposed scheme is close to the fully connected one after just a few iterations performed at the digital domain.

Index Terms — hybrid multi-user equalizer, massive MIMO, millimeter-wave communications, hybrid sub-connected analog-digital architectures.

I. INTRODUCTION

The combination of millimeter wave (mmWave) with massive MIMO (mMIMO), when compared to the current sub-6 GHz communication systems, is very attractive because the smaller wavelength allows to pack more antennas in the same volume [1], and mmWave mMIMO also offers more degrees of freedom [2]. However, the power consumption and high cost of some mixed-signal components makes unpractical to implement one fully dedicated radio frequency (RF) chain by transmit/receive antenna [3] as in sub-6 GHz MIMO systems [4].

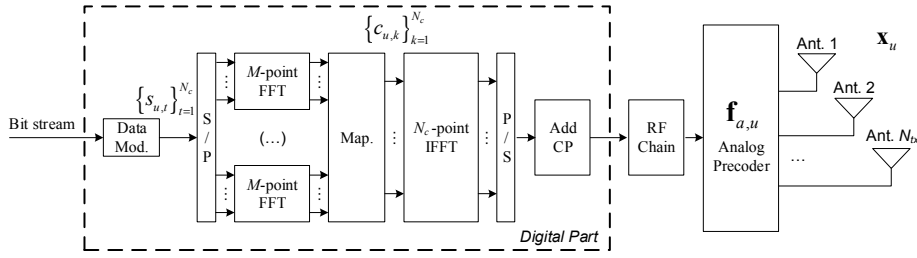
A simple approach to solve this problem is the use of only phase shifters implementing a fully analog beamforming technique, but the performance is limited, and it is typically applied in a single-stream transmission [5]. Therefore some hybrid analog-digital architectures were proposed, where some signal processing is firstly done in the analog domain, and then a lower complexity processing is done in the digital domain [6]. There are fully-connected hybrid architectures, where each RF chain is connected to all transmit or receive antennas but that may require a large number of

connections, and subconnected hybrid architectures, where each RF chain is only connected to a subset of antennas [7]. Fully connected hybrid architectures were addressed in [8][9]. In [8], it was proposed a precoder to multiuser narrowband systems, where a spatial rotation to reduce the number of the RF chains required by user was employed. Then, using the angles of arrivals of each user, they are scheduled by an angle division multiple access scheme. The authors of [9] proposed a precoder to single-user wideband systems, where the digital precoding can be different for each subcarrier, but with a frequency flat analog precoding. Sub-connected hybrid architectures were addressed in [7],[10][11]. In [7], it is proposed, for a single-user narrowband system, a precoder to maximize the total achievable data rate, where first the analog part is designed for two cases, high and low signal-to-noise ratio (SNR), and then the digital part is obtained by waterfilling algorithm. In [10], the authors designed a precoder /combiner for single user a broadband system, where the over-all spectral efficiency is maximized by considering a power budget constraint for each subcarrier. The authors of [11] proposed a precoder for downlink multiuser narrowband system where the analog precoder is built using the partial information of the conjugate transposed of channel matrix, and then it is applied a ZF precoder in the digital part to remove the interference.

It is well known that the use of nonlinear equalizers is more efficient to remove the multiuser/inter-symbol interference [12] and therefore we use this principle to design the digital part of the proposed hybrid equalizer for sub-connected mmWave mMIMO MIMO single carrier frequency division multiple access (SC-FDMA) systems. We consider a two-step hybrid multiuser equalizer, where the digital part is computed iteratively but the analog part is kept constant over the iterations. The limitation that each RF chain is only physically connected to a sub-set of antennas makes the design of the proposed sub-connected hybrid iterative multiuser equalizer harder than for the fully connected based approach. The BER performance of the proposed tends to the BER performance of a fully connected hybrid equalizer as the number of iterations increases.

The remainder of this paper is organized as follows: in Section II is defined the system model assumed in this paper. In Section III is presented the fully analog precoder employed at each user terminal (UT). Then, in Section IV we design the proposed two-step hybrid broadband multi-user

This work is supported by the European Regional Development Fund (FEDER), through the Competitiveness and Internationalization Operational Program (COMPETE 2020) of the Portugal 2020 framework, Regional OP Centro (CENTRO 2020), Regional OP Lisboa (LISBOA 14-20) and by FCT/MEC through national funds, under Project MASSIVE5G (AAC n° 02/SAICT/2017) and project UID/EEA/50008/2013.


 Fig 1. Block diagram of the u th UT.

equalizer. Finally, the main performance results is shown in Section V and the conclusions in section VI.

II. SYSTEM MODEL CHARACTERIZATION

We consider a SC-FDMA uplink mmWave system, with N_c available subcarriers, U users sharing the same radio resources, with one RF chain and N_{tx} transmit antennas, where each user sends one data stream per subcarrier. The base station has R RF chains by each antenna, with a total of N_{rx}^{RF} RF chains and $N_{rx} = RN_{rx}^{RF}$ receive antennas, where $U \leq N_{rx}^{RF} \leq N_{rx}$. We consider a clustered channel with N_{cl} clusters, and N_{ray} paths per cluster. The channel matrix is denoted by $\mathbf{H}_{u,k} \in \mathbb{C}^{N_{rx} \times N_{tx}}$ in the frequency domain to the k th subcarrier and u th user, and it is given by

$$\mathbf{H}_{u,k} = \sum_{d=0}^{D-1} \mathbf{H}_{u,d} e^{-j \frac{2\pi k d}{N_c}}, \quad (1)$$

with

$$\mathbf{H}_{u,d} = \sqrt{\frac{N_{rx} N_{tx}}{\rho_{PL}}} \sum_q \sum_l \left(\alpha_{q,l}^u p_{rc}(dT_s - \tau_q^u - \tau_{q,l}^u) \right) \times \mathbf{a}_{tx,u}(\theta_q^u - \vartheta_{q,l}^u) \mathbf{a}_{rx,u}^H(\phi_q^u - \varphi_{q,l}^u), \quad (2)$$

where ρ_{PL} is the path-loss from the transmitter to the receiver and $\alpha_{q,l}^u$ is the complex path gain at the l th ray of the q th cluster. The function $p_{rc}(\cdot)$ is the pulse shaping function where the raised-cosine filter was adopted, with the spaced signaling, T_s , as in [15]. The time delay of q th cluster is τ_q^u , and the angles of departure and arrival are θ_q^u and ϕ_q^u , respectively. The relative time delay, relative angles of arrival and departure of the l th ray of the q th cluster are $\tau_{q,l}^u$, $\vartheta_{q,l}^u$, and $\varphi_{q,l}^u$, respectively. The paths delay have a uniform distribution in $[0, DT_s]$ and the angles have a random distribution presented in [15], such that $\mathbb{E}[\|\mathbf{H}_{u,d}\|_F^2] = N_{rx} N_{tx}$. Lastly, the vector $\mathbf{a}_{rx,u}$ and $\mathbf{a}_{tx,u}$ are the normalized receive and transmit array response vectors, respectively.

The received signal is given, at the k th subcarrier, by

$$\mathbf{y}_k = \sum_{u=1}^U \mathbf{H}_{u,k} \mathbf{x}_{u,k} + \mathbf{n}_k, \quad (3)$$

where $\mathbf{n}_k \in \mathbb{C}^{N_{rx}}$ is the zero mean Gaussian noise with variance σ_n^2 and $\mathbf{x}_{u,k} \in \mathbb{C}^{N_{tx}}$ is the transmit complex baseband signal of the u th user at subcarrier k .

III. TRANSMITTER DESIGN

In this section, we design the proposed low-complex analog precoders employed at the UTs. The block diagram of the u th UT is shown in Fig 1. It is assumed only QPSK constellations from where is selected the data symbol $s_{u,t}$, with $\mathbb{E}[|s_{u,t}|^2] = \sigma_u^2$. The extension to other constellations can be obtained directly. The sequence $\{s_{u,t}\}_{t=1}^{N_c}$ is divided into S data blocks of size $M = N_c / S$, where $\{c_{u,k}\}_{k=(r-1)M+1}^{rM}$, $c_{u,k} \in \mathbb{C}$, is the DFT of $\{s_{u,t}\}_{t=(r-1)M+1}^{rM}$, $r = 1, \dots, S$. Without loss of generality, we assume that $M = N_c$. Lastly, the cyclic prefix (CP) is added on each RF chain.

The transmitter processing has two parts, an analog processing and a digital baseband processing. At the digital part is applied a SC-FDMA encoding, and at the analog part, it is only used analog phase shifters with constant amplitude, due hardware constraints, which implies all vector elements of $\mathbf{f}_{a,u} \in \mathbb{C}^{N_{tx}}$ to have the same norm ($|\mathbf{f}_{a,u}(n)|^2 = N_{tx}^{-1}$). To find the analog precoder, firstly the correlation matrix $\mathbf{A}_{tx,u} \mathbf{A}_{tx,u}^H$ is computed, where

$$\mathbf{A}_{tx,u} = [\mathbf{a}_{tx,u}(\theta_1^u), \dots, \mathbf{a}_{tx,u}(\theta_j^u), \dots, \mathbf{a}_{tx,u}(\theta_{N_{cl}}^u)] \in \mathbb{C}^{N_{tx} \times N_{cl}}, \quad (4)$$

and then the singular value decomposition is applied to $\mathbf{A}_{tx,u} \mathbf{A}_{tx,u}^H = \mathbf{\Lambda}_{tx,u} \mathbf{\Sigma}_{tx,u} \mathbf{\Lambda}_{tx,u}^H$. The goal is to point the beams along the dominant directions of $\mathbf{H}_{u,k}$. Therefore, at the u th UT, the analog precoder matrix is

$$\mathbf{f}_{a,u}(n) = \frac{1}{\sqrt{N_{tx}}} \exp\{j \arg(\mathbf{\Lambda}_{tx,u}(n,1))\}, 1 \leq n \leq N_{tx}. \quad (5)$$

Finally, the discrete transmitted baseband signal of the u th user, at subcarrier k , $\mathbf{x}_{u,k} \in \mathbb{C}^{N_{tx}}$ is given by

$$\mathbf{x}_{u,k} = \mathbf{f}_{a,u} c_{u,k}. \quad (6)$$

IV. RECEIVER DESIGN

In this section we design a sub-optimal two-step approach, with a hybrid receiver structure, where firstly is designed the analog part of the equalizer and then it is computed the iterative digital part to further remove the interference. It is assumed that the RF analog equalizer is the same over the bandwidth, which means that it has no frequency selectivity. Therefore, it is equivalent to apply the RF analog equalizer in the time or frequency domain. Besides, the analog equalizer is also assumed constant between iterations because it is not feasible to store the receive signal

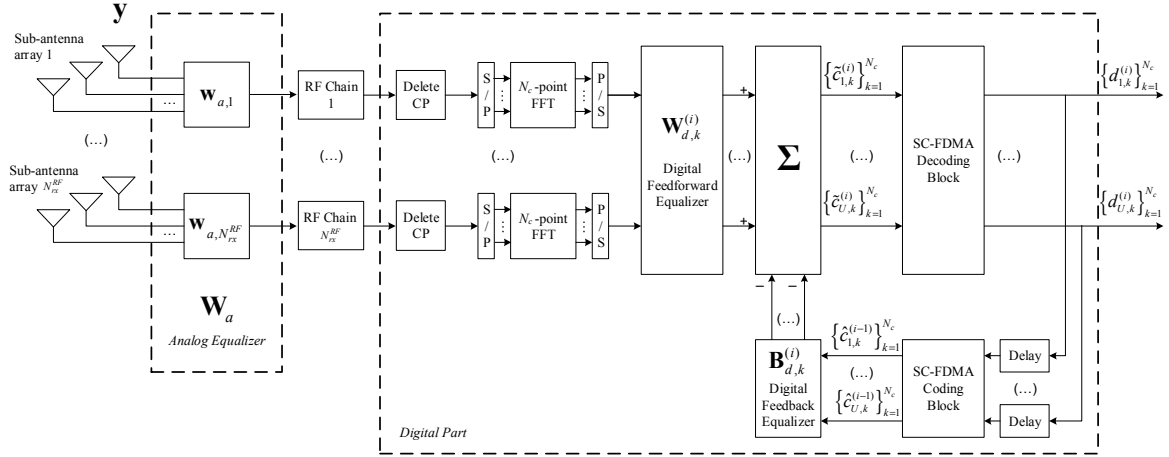


Fig 2. Block diagram of BS.

in analog domain to apply fully analog-digital iterative processing.

The proposed hybrid N_c -length block space-frequency broadband decoder is shown in Fig. 2. At the k th subcarrier, the received signal for iteration i , $\tilde{\mathbf{c}}_k^{(i)} = \{\tilde{c}_{u,k}^{(i)}\}_{u=1}^U \in \mathbb{C}^U$, is given by

$$\tilde{\mathbf{c}}_k^{(i)} = \mathbf{W}_{d,k}^{(i)} \mathbf{W}_a \mathbf{y}_k - \mathbf{B}_{d,k}^{(i)} \hat{\mathbf{c}}_k^{(i-1)}, \quad (7)$$

where $\mathbf{W}_a \in \mathbb{C}^{N_{rx}^{RF} \times N_{rx}}$ is the analog equalizer diagonal matrix, $\mathbf{W}_{d,k}^{(i)} \in \mathbb{C}^{U \times N_{rx}^{RF}}$ and $\mathbf{B}_{d,k}^{(i)} \in \mathbb{C}^{U \times U}$ are the digital feedforward and feedback matrices, respectively. The received signal, \mathbf{y}_k , is initially processed through the analog phase shifters, with $|\mathbf{W}_a(r, l)|^2 = R^{-1}$ to $R(r-1)+1 \leq l \leq Rr$ and $|\mathbf{W}_a(r, l)|^2 = 0$ to the other entries, and then it is applied a baseband processing, composed by N_{rx}^{RF} RF chains and the iterative digital equalizer. In the forward path of the digital equalizer, it is applied a linear filter $\mathbf{W}_{d,k}^{(i)} \in \mathbb{C}^{U \times N_{rx}^{RF}}$ used at subcarrier k , then the SC-FDMA decoding and finally the data demodulation. In the feedback path, the data recovered from the forward path is again modulated and SC-FDMA encoded. Then, it is applied the feedback matrix $\mathbf{B}_{d,k}^{(i)} \in \mathbb{C}^{U \times U}$ at k th subcarrier. It can be proven that the feedback matrix that minimize the $\text{MSE}_k^{(i)} = \mathbb{E}[\|\tilde{\mathbf{c}}_k^{(i)} - \mathbf{c}_k\|^2]$, with $\mathbf{c}_k = \{\mathbf{c}_{u,k}\}_{u=1}^U \in \mathbb{C}^U$, is given by

$$(\mathbf{B}_{d,k}^{(i)})_{opt} = ((\mathbf{W}_{d,k}^{(i)})_{opt} \mathbf{W}_a \mathbf{H}_k - \mathbf{I}_U) (\boldsymbol{\Psi}^{(i-1)})^H, \quad (8)$$

where $\mathbf{H}_k = [\mathbf{H}_{u,k} \mathbf{f}_{a,u}]_{1 \leq u \leq U} \in \mathbb{C}^{N_{rx} \times U}$. Therefore, the simplified optimization problem can be formulated as,

$$\begin{aligned} ((\mathbf{W}_a)_{opt}, (\mathbf{W}_{d,k}^{(i)})_{opt}) &= \arg \min \sum_{k=1}^{N_c} \overline{\text{MSE}}_k^{(i)} \\ \text{s.t. } \sum_{k=1}^{N_c} \text{diag}(\mathbf{W}_{d,k}^{(i)} \mathbf{W}_a \mathbf{H}_k) &= N_c \mathbf{I}_U, \quad (9) \\ \mathbf{W}_a &\in \mathcal{W}_a. \end{aligned}$$

where $\overline{\text{MSE}}_k^{(i)}$ represents the MSE between the hybrid analog-digital equalizer $\mathbf{W}_{d,k}^{(i)} \mathbf{W}_a$ we want to compute and the fully digital equalizer $(\overline{\mathbf{W}}_{ad,k}^{(i)})_{opt}$ given by

$$\overline{\text{MSE}}_k^{(i)} = \left\| \left(\mathbf{W}_{d,k}^{(i)} \mathbf{W}_a - (\overline{\mathbf{W}}_{ad,k}^{(i)})_{opt} \right) (\tilde{\mathbf{R}}_k^{(i-1)})^{1/2} \right\|_F^2, \quad (10)$$

with

$$(\overline{\mathbf{W}}_{ad,k}^{(i)})_{opt} = (\mathbf{I}_U - |\boldsymbol{\Psi}^{(i-1)}|^2) \mathbf{H}_k^H (\tilde{\mathbf{R}}_k^{(i-1)})^{-1}, \quad (11)$$

$$\tilde{\mathbf{R}}_k^{(i-1)} = \mathbf{H}_k (\mathbf{I}_U - |\boldsymbol{\Psi}^{(i-1)}|^2) \mathbf{H}_k^H + \sigma_n^2 \sigma_u^{-2} \mathbf{I}_U. \quad (12)$$

where \mathcal{W}_a is the set of feasible analog equalizers and $\tilde{\mathbf{R}}_k^{(i)}$ represents the received signal correlation matrix. It can be shown that the $\overline{\text{MSE}}$ is up to a constant equal to MSE . The diagonal matrix, $\boldsymbol{\Psi}^{(i)}$, whose u th diagonal element, associated with the iteration $i-1$, gives a blockwise reliability measure of the u th user data block estimates, can be written as [14],

$$\boldsymbol{\Psi}^{(i)} = \text{diag}(\psi_1^{(i)}, \dots, \psi_u^{(i)}, \dots, \psi_U^{(i)}), \quad (13)$$

where each coefficient is given by

$$\psi_u^{(i)} = \frac{\mathbb{E}[\hat{c}_{u,k}^{(i)} c_{u,k}^{*}]^2}{\mathbb{E}[|c_{u,k}|^2]}, \quad u \in \{1, \dots, U\}. \quad (14)$$

The matrices $\boldsymbol{\Psi}^{(i)}$, $i \geq 1$ can only be computed after to obtain the data estimate, $\hat{\mathbf{c}}_k^{(i)}$, and consequently after to obtain the equalizer matrices. Therefore, to compute the analog equalizer \mathbf{W}_a , it is assumed that $\boldsymbol{\Psi}^{(0)} = \mathbf{0}_U$, because there is not available information about the data estimate. To ensure the constraint $\mathbf{W}_a \in \mathcal{W}_a$, the matrix \mathbf{W}_a is built using a receive response vectors based dictionary. This dictionary, $\mathbf{A}_{rx}^r \in \mathbb{C}^{N_{rx} \times N_d N_{ray}}$, is given by

$$\mathbf{A}_{rx}^r(n, l) = \begin{cases} \mathbf{A}_{rx,u}(n, l), & R(r-1)+1 \leq n \leq Rr \\ & 1 \leq l \leq N_d N_{ray} \\ 0, & \text{otherwise} \end{cases}, \quad (15)$$

where $\mathbf{A}_{rx,u} = [\mathbf{a}_{rx,u}(\theta_{1,1}^{rx,u}), \dots, \mathbf{a}_{rx,u}(\theta_{N_d, N_{ray}}^{rx,u})] \in \mathbb{C}^{N_{rx} \times N_d N_{ray}}$, with the data of u th user associated to the r th RF chain, and

Algorithm 1: Fixed analog equalizer

1: $\mathbf{W}_a = \text{Empty Matrix}$
2: $\mathbf{W}_{res,k} = -\mathbf{H}_k^H$
3: $\tilde{\mathbf{R}}_k = \mathbf{H}_k \mathbf{H}_k^H + \sigma_n^2 \sigma_u^{-2} \mathbf{I}_U$
4: **for** $r = 1, \dots, N_{rx}^{RF}$ **do**
5: $\Lambda_k = \mathbf{W}_{res,k} \left(\mathbf{A}_{rx}^r \right) \left(\left(\mathbf{A}_{rx}^r \right)^H \tilde{\mathbf{R}}_k \left(\mathbf{A}_{rx}^r \right) \right)^{-1/2}$
6: $n_{opt} = \arg \max_{l=1, \dots, N_{CB}} \left[\sum_{k=1}^{N_c} \left| \Lambda_k^H \Lambda_k \right| \right]_l$
7: $\mathbf{W}_a = \left[\mathbf{W}_a^H \mid \left(\mathbf{A}_{rx}^r \right)^{n_{opt}} \right]^H$
8: $\mathbf{W}_{res,k} = \Omega_d \mathbf{H}_k^H \mathbf{W}_a^H \left(\mathbf{W}_a \tilde{\mathbf{R}}_k \mathbf{W}_a^H \right)^{-1} \mathbf{W}_a \tilde{\mathbf{R}}_k$
 $- \Omega_d \mathbf{H}_k^H$
9: **end for**
10: **return** \mathbf{W}_a

$n = 1, \dots, N_{rx}$ is the receive antenna index. From the KKT conditions used to solve (9), we obtain the residue matrix $\mathbf{W}_{res,k}^{(i)} \in \mathbb{C}^{U \times N_{rx}}$ given by

$$\mathbf{W}_{res,k}^{(i)} = \mathbf{W}_{d,k}^{(i)} \mathbf{W}_a \left(\tilde{\mathbf{R}}_k^{(i-1)} \right) - \Omega_d \mathbf{H}_k^H, \quad (16)$$

where

$$\Omega_d = N_c \left(\sum_{k=1}^{N_c} \text{diag} \left(\left(\mathbf{W}_{d,k}^{(i)} \right)_{opt} \left(\mathbf{W}_a \right)_{opt} \mathbf{H}_k \right) \right)^{-1}. \quad (17)$$

forces the power constraint of problem (9). Considering that $\Psi^{(0)} = \mathbf{0}_U$, the residue matrix reduces to $\mathbf{W}_{res,k} = -\mathbf{H}_k^H$. It can also be proven that the digital feedforward equalizer as a function of a given analog equalizer matrix \mathbf{W}_a is

$$\left(\mathbf{W}_{d,k}^{(i)} \right)_{opt} \left[\mathbf{W}_a \right] = \Omega_d \mathbf{H}_k^H \mathbf{W}_a \left(\mathbf{W}_a \tilde{\mathbf{R}}_k^{(i-1)} \left(\mathbf{W}_a \right)^H \right)^{-1}. \quad (18)$$

The pseudo-code to compute the coefficients of analog part of the equalizer is given by Algorithm 1. To compute the analog equalizer, after initializing the necessary matrices (lines 1-3), we have a loop that selects one vector of the dictionary at each iteration, until a total of N_{rx}^{RF} vectors. In lines 5, 6 the vector is selected and then added to \mathbf{W}_a in line 7, and its effect removed in line 8. In Algorithm 2, the iterative digital equalizers are computed using \mathbf{W}_a obtained from Algorithm 1, where i_{\max} is the maximum number of iterations. Firstly, the matrices are initialized (lines 1-2), then the digital feedforward equalizer (line 4), and the feedback equalizer (line 5) are computed. Finally, the matrices $\Psi^{(i)}$ and $\tilde{\mathbf{R}}_k^{(i)}$ are updated, at lines 6 and 7, respectively.

V. PERFORMANCE RESULTS

The performance of the proposed sub-connected hybrid analog-digital multiuser equalizer is discussed in this section. We consider, for each user, a clustered wideband chan-

Algorithm 2: Iterative digital equalizer

Input: \mathbf{W}_a
1: $\Psi^{(0)} = \mathbf{0}_U$
2: $\tilde{\mathbf{R}}_k^{(0)} = \mathbf{H}_k \left(\mathbf{I}_U - \left| \Psi^{(0)} \right|^2 \right) \mathbf{H}_k^H + \sigma_n^2 \sigma_u^{-2} \mathbf{I}_U$
3: **for** $i = 1, \dots, i_{\max}$ **do**
4: $\left(\mathbf{W}_{d,k}^{(i)} \right)_{opt} = \Omega_d \mathbf{H}_k^H \mathbf{W}_a^H \left(\mathbf{W}_a \tilde{\mathbf{R}}_k^{(i-1)} \mathbf{W}_a^H \right)^{-1}$
5: $\left(\mathbf{B}_{d,k}^{(i)} \right)_{opt} = \left(\left(\mathbf{W}_{d,k}^{(i)} \right)_{opt} \mathbf{W}_a \mathbf{H}_k - \mathbf{I}_U \right) \left(\Psi^{(i-1)} \right)^H$
6: **Compute** $\Psi^{(i)}$
7: $\tilde{\mathbf{R}}_k^{(i)} = \mathbf{H}_k \left(\mathbf{I}_U - \left| \Psi^{(i)} \right|^2 \right) \mathbf{H}_k^H + \sigma_n^2 \sigma_u^{-2} \mathbf{I}_U$
8: **end for**
9: **return** $\left(\mathbf{W}_{d,k}^{(i)} \right)_{opt}, \left(\mathbf{B}_{d,k}^{(i)} \right)_{opt}$

nel model with $N_{cl} = 4$ clusters and $N_{ray} = 5$ rays per cluster, where the azimuth angles of departure (θ_j^u) and arrival (θ_j^r) have Laplacian distribution. We assumed that the all N_{cl} clusters have same the average power and an angle spread equal to 10° degrees at the transmitter and receiver. We considered uniform linear arrays (ULAs), although this hybrid receiver configuration can be applied to other antenna array configurations. The carrier frequency is set to 72 GHz and the antenna element spacing is half-wavelength. It is used $N_c = 128$ subcarriers and the CP is equal to $D = N_c / 4 = 32$. We assumed perfect CSI knowledge and synchronization at the receiver side.

We present results in Fig. 3, for a scenario whose the parameters are $U = N_{rx}^{RF} = 8$, $N_{rx} = 16$, $N_{rx} = 32$. Then, it is evaluated the performance when the parameter $R = N_{rx} / N_{rx}^{RF}$ changes, in Fig. 4. It is considered the BER as the performance metric as function of the E_b / N_0 , where E_b is the average bit energy and N_0 is the one-sided noise power spectral density. The transmitted signal of all users have the same power, i.e., $\sigma_1^2 = \dots = \sigma_U^2 = 1$, and it is considered an identical the average E_b / N_0 for all with $E_b / N_0 = \sigma_u^2 / (2\sigma_n^2) = \sigma_n^{-2} / 2$.

Starting with the results of Fig. 3, we show the performance for iteration 1, 2, 3 and 4 of the proposed hybrid sub-connected equalizer with the designed analog precoder and we can see that this one improves as the number of iterations increases as expected. Additionally, the gaps between the 1st and 2nd iterations are much higher than between the 3rd and 4th iterations. This occurs because most of the residual inter symbol and multiuser interferences are removed from the 1st to the 2nd iteration. When compared with the hybrid fully connected counterpart, at a target BER of 10^{-3} , the penalties are approximately 4dB for iteration 1, but only 0.8dB for iteration 4. This means that the iterative digital approach for sub-connected architectures is quite efficient

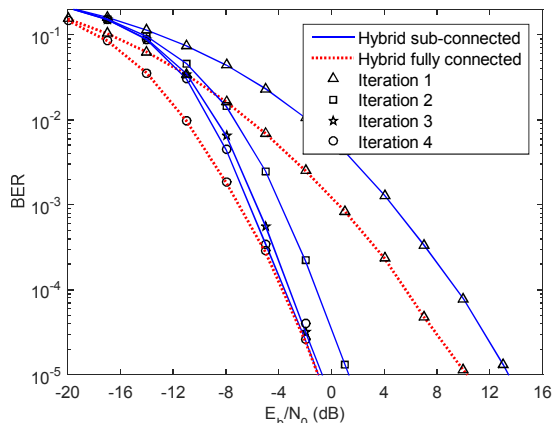


Fig 3. Performance comparison of the proposed hybrid sub-connected equalizer with the hybrid fully connected and fully digital

because the performance is closer of performance of the hybrid fully connected counterpart with only four iterations. We can also observe that for high E_b/N_0 regime the performance of both architectures are approximately the same for the 4th iteration.

In Fig. 4, we present results for different values of $R = 2, 4, 8$ and for iteration 1 and 4. We also added the curve for fully digital approach which corresponds to $R = 1$. As it can be seen for the first iteration (linear digital equalizer) the performance for all R s is basically the same. However, for the 4th iteration the performance improves as R decreases despite the number of users increases. This happens because the sub-connected systems tends to the fully digital one as the number of RFs chains increases and the proposed hybrid equalizer has more degrees of freedom to efficiently to remove the additional multi-user interference. It can be observed for the 4th iteration and a BER of 10^{-3} a penalty against the fully digital ($R = 1$) of 1.9dB, 4.2dB and 6.9dB for $R=2, 4$ and 8 , respectively.

VI. CONCLUSIONS

We designed a two-step hybrid multiuser equalizer for a sub-connected mmWave massive MIMO architecture, where the analog part is constant over the sub-carriers and the digital one computed iteratively. We also considered low-complexity UTs employing a simple but quite efficient AoD based precoder. Firstly, it was verified that the proposed hybrid iterative multiuser equalizer converges and that it achieves a performance close to the hybrid fully connected counterpart, requiring only a few iterations. We also saw that the performance tends to the one obtained with fully digital approach when the number of RF chains increases. Therefore, the proposed receiver structure combined with the low complexity analog precoder is interesting for practical mmWave massive MIMO based systems, since it ensures good performance at a low cost.

REFERENCES

- [1] T. Vu et. al., "Ultra-Reliable and Low Latency Communication in mmWave-Enabled Massive MIMO Networks", *IEEE Commun. Letters*, vol. 5, pp. 170 - 182, Dec. 2016.
- [2] J. Huang, C. Wang, R. Feng, J. Sun, W. Zhang, and Y. Yang, "Multi-Frequency MmWave Massive MIMO Channel Measurements and

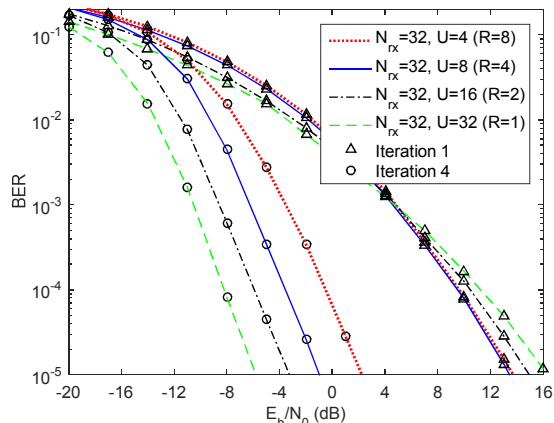


Fig 4. Performance comparison of the proposed hybrid sub-connected equalizer to different R s.

Characterization for 5G Wireless Communication Systems," *IEEE J. Sel. Areas Commun.*, vol. PP, no. 99, pp. 1–1, April 2017.

- [3] A. Rozé, M. Crussière, M. Héland, and C. Langlais, "Comparison between a hybrid digital and analog beamforming system and a fully digital Massive MIMO system with adaptive beamsteering receivers in millimeter-Wave transmissions," *Intern. Symp. on Wireless Commun. Systems*, vol. 2016, pp. 1–1, Sep. 2016.
- [4] M. Agiwal, A. Roy, and N. Saxena, "Next Generation 5G Wireless Networks: A Comprehensive Survey," *IEEE Commun. Surveys & Tutorials*, vol. 18, no. 3, pp. 1617 - 1655, Feb. 2016.
- [5] R. W. Heath, N. Gonzalez-Prelcic, S. Rangan, W. Roh, and A. M. Sayeed, "An overview of signal processing techniques for millimeter wave MIMO systems," *IEEE J. Sel. Topics Signal Process.*, vol. 10, no. 3, pp. 436–453, Apr. 2016.
- [6] O. El Ayach, S. Rajagopal, S. Surra, Z. Pi, and R. W. Heath, Jr., "Spatially Sparse Precoding in millimeter wave MIMO systems", *IEEE Trans. Wireless Commun.* vol. 13, no. 3, pp. 1499–1513, Mar. 2014.
- [7] N. Li, Z. Wei, H. Yang, X. Zhang, and D. Yang, "Hybrid Precoding for mmWave Massive MIMO Systems With Partially Connected Structure," *IEEE Access*, vol.5, pp. 15142 - 15151, Jun. 2017
- [8] J. Zhao, F. Gao, W. Jia, S. Zhang, S. Jin, and Hai Lin, "Angle Domain Hybrid Precoding and Channel Tracking for Millimeter Wave Massive MIMO Systems," *IEEE Trans. on Wireless Commun.*, vol.16, no. 10, pp. 6868 - 6880, Aug. 2017.
- [9] A. Alkhateeb, and R. W. Heath, "Frequency Selective Hybrid Precoding for Limited Feedback Millimeter Wave Systems", *IEEE Trans. Commun.* vol. 64, no. 5, pp. 1801 - 1818, 2016.
- [10] F. Sohrabi, and W. Yu, "Hybrid Analog and Digital Beamforming for OFDM-Based Large-Scale MIMO Systems," *Signal Processing Advances in Wireless Commun. (SPAWC)*, vol. 2016, pp. 1-1, July, 2016.
- [11] Y. Guo, L. Li, X. Wen, W. Chen, and Z. Han, "Sub-array Based Hybrid Precoding Design for Downlink Millimeter-Wave Multi-User Massive MIMO Systems," *International Conference on Wireless Commun. and Signal Processing (WCSP)*, vol.2017, pp. 1-1, Oct. 2017
- [12] N. Benvenuto, R. Dinis, D. Falconer, and S. Tomasin, "Single carrier modulation with non linear frequency domain equalization: An idea whose time has come - Again," *Proceedings of the IEEE*, vol. 98, no. 1, pp. 69-96, Jan. 2010.
- [13] H. E. Rowe, "Memoryless nonlinearities with Gaussian inputs: elementary results," *Bell Syst. Tech. J.*, vol. 61, no. 7, pp.1519-1525, 1982.
- [14] A. Silva, J. Assunção, R. Dinis, and A. Gameiro, "Performance evaluation of IB-DFE- based strategies for SC-FDMA systems," *EURASIP Journal on Wireless Commun. and Networking*, Vol. 2013, No. 1, pp. 1 - 10, Dec., 2013
- [15] Ahmed Alkhateeb, and Robert W. Heath, "Frequency Selective Hybrid Precoding for Limited Feedback Millimeter Wave Systems", *IEEE Trans. Commun.* vol. 64, no. 5, pp. 1801 - 1818, 2016.